

Reflection High Energy Electron Diffraction and Atomic Force Microscopy Studies of $\text{Mn}_x\text{Sc}_{(1-x)}$ Alloys Grown on MgO(001) Substrates by Molecular Beam Epitaxy

Costel Constantin,¹ Abhijit Chinchore,² Arthur R. Smith,²

¹Department of Physics and Astronomy, James Madison University, Harrisonburg, VA 22801

²Nanoscale & Quantum Phenomena Institute, Department of Physics and Astronomy, Ohio University, Athens, OH 45701

ABSTRACT

The combination of the molecular beam epitaxy growth method with the *in-situ* reflection high energy electron diffraction measurements currently offers unprecedented control of crystalline growth materials. We present here a stoichiometric study of $\text{Mn}_x\text{Sc}_{(1-x)}$ [$x = 0, 0.03, 0.05, 0.15, 0.25, 0.35, \text{ and } 0.50$] thin films grown on MgO(001) substrates with this growth method. Reflection high energy electron diffraction and atomic force microscopy measurements reveal alloy behavior for all of our samples. In addition, we found that samples $\text{Mn}_{0.10}\text{Sc}_{0.90}$ and $\text{Mn}_{0.50}\text{Sc}_{0.50}$ display surface self-assembled nanowires with a length/width ratio of $\sim 800 - 2000$.

INTRODUCTION

Due the fact that manganese is a sulfur-fixing agent and thus helps increase the corrosion resistance in steel production, there is a significant interest in alloying it with iron, vanadium, chromium, and aluminum [1-6]. To date, very few groups have explored the possibility of alloying manganese with scandium [e.g., Ref. 7]. Buch *et al.* [7] reported that the Mn_2Sc alloy enhances the creep resistance of magnesium alloys only above 450 °C. The increase in the creep resistance found in this study has been attributed to a semi-coherent precipitation formed by the Mn_2Sc inside the magnesium alloy grains. The phase diagram for Mn-Sc alloys have been reviewed recently [8, 9], with the conclusion that the $\text{Mn}_{23}\text{Sc}_6$, Mn_2Sc , and MnSc_4 were the most stable; however, only Mn_2Sc melted congruently, while the other two formed peritectic reaction. Mn-Sc alloys are usually synthesized in bulk by normal crucible melting and levitation melting methods [10]. This material has never been synthesized by radio-frequency molecular beam epitaxy (rf-MBE). We show here that $\text{Mn}_x\text{Sc}_{(1-x)}$ thin films can be grown with this method with a stoichiometry range from $x = 0$ to $x = 0.5$. We present here a preliminary analysis of the way in which different stoichiometries influence surface properties, including growth of surface self-assembled nanowires.

EXPERIMENT

We performed the growth of Mn-Sc alloys using a homemade rf-MBE growth chamber [11, 12] and we employed Knudson effusion cells for manganese and scandium metallic sources. Before we loaded the MgO(001) substrates into the rf-MBE chamber, we ultrasonically cleaned them with acetone and isopropanol. Inside the chamber the substrates were deoxidized by heating and nitridation at a temperature of 900 °C for 30 minutes, by keeping the N_2 flow rate to 1.1 sccm ($P_{\text{chamber}} = 9 \times 10^{-6}$ Torr) and rf-plasma power of 500 W. All the films were grown with

a thickness of ~ 50 nm each, and at a substrate temperature of $T_s \sim 450$ °C. The T_s was measured *in-situ* with a thermocouple located behind the substrate heater. This value was verified *ex-situ* with an infrared pyrometer pointed through a glass window directly at the front side of the sample. The fractional concentrations x for $Mn_xSc_{(1-x)}$ were varied between 0 and 0.5. The concentrations are given by the flux ratio $x = J_{Mn} / (J_{Mn} + J_{Sc})$, with $J_{Sc} = 1.5 \times 10^{14}$ cm⁻²s⁻¹, and $J_{Mn} \sim 4.64 \times 10^{12}$ cm⁻²s⁻¹ - 2×10^{14} cm⁻²s⁻¹. The growths were monitored *in-situ* by reflection high energy electron diffraction (RHEED) by using a 20 keV electron-beam, and the films were measured *ex-situ* by atomic force microscopy (AFM).

RESULTS AND DISCUSSIONS

In the following we discuss here the RHEED and AFM measurements of $Mn_xSc_{(1-x)}$ thin films with a focus on eight stoichiometric ratios: Sc, $Mn_{0.03}Sc_{0.97}$, $Mn_{0.05}Sc_{0.95}$, $Mn_{0.10}Sc_{0.90}$, $Mn_{0.15}Sc_{0.85}$, $Mn_{0.25}Sc_{0.75}$, $Mn_{0.35}Sc_{0.65}$, and $Mn_{0.50}Sc_{0.50}$. These stoichiometric choices are based on previous experience with MnScN thin film growth that suggests the existence of ferromagnetism at room temperature [13].

RHEED results

In Figure 1(α) and 1(β) we present RHEED patterns for MgO(001) substrates immediately after they had been deoxidized. Figures 1(α) and 1(β) look streaky indicating a smooth, 2-dimensional surface, which constitutes a good nucleation surface for the subsequent $Mn_xSc_{(1-x)}$ thin film growth.

At the end of the $Mn_xSc_{(1-x)}$ film growths we recorded the RHEED patterns presented in Figure 1 (a – h). These patterns were taken in the same crystal orientation as for the MgO(001) substrate. The surface of Sc film [Figure 1 (a)] shows a rather spotty, diffuse, and ring-like pattern. The spotty behavior indicates a 3-dimensional growth mode; whereas the diffuse and ring-like behavior suggests that the individual Sc growth grains are randomly oriented relative to each other (i.e., polycrystalline behavior). Polycrystalline materials have short range but no long range atomic order. The patterns for $Mn_{0.03}Sc_{0.97}$ and $Mn_{0.05}Sc_{0.95}$ films show somehow a streakier behavior [Figures 1(b) and 1(c)], indicating a more 2-dimensional growth as compared to the growth of Sc [Figure 1(a)]. Moreover, the pattern gets improved for $Mn_{0.10}Sc_{0.90}$ [Figure 1(d)], but for $Mn_{0.15}Sc_{0.85}$ film the pattern deteriorates into a diffuse one [Figure 1(e)]. Nevertheless, the best patterns we measured for this entire study can be seen for $Mn_{0.25}Sc_{0.75}$, and $Mn_{0.35}Sc_{0.65}$ films [Figures 1(f) and 1(g)]. For $Mn_{0.50}Sc_{0.50}$ film, the pattern [Figure 1(h)] looks heavily spotty and ring-like behavior indicating a 3-dimensional and polycrystalline growth mode. Based on our RHEED measurements presented above, we can say that all of our films exhibit alloy behavior. However, we observed single crystal growth only for samples $Mn_{0.03}Sc_{0.97}$, $Mn_{0.05}Sc_{0.95}$, $Mn_{0.10}Sc_{0.90}$, $Mn_{0.25}Sc_{0.75}$, and $Mn_{0.35}Sc_{0.65}$, respectively.

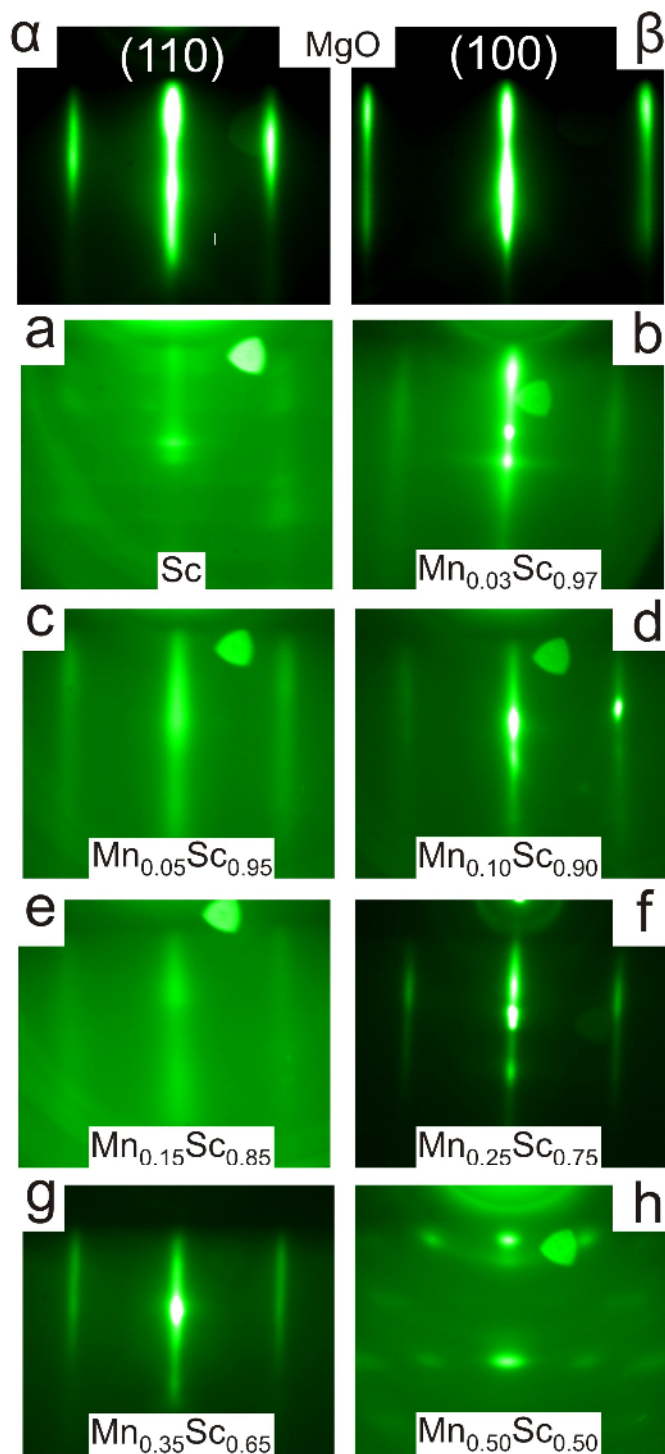


Figure 1. (α) & (β) RHEED patterns of MgO(001) substrate taken before the $\text{Mn}_x\text{Sc}_{(1-x)}$ film growth. (a) – (h) RHEED patterns for $\text{Mn}_x\text{Sc}_{(1-x)}$ at various x compositions ($0 \leq x \leq 0.5$). Note that (α) & (β) RHEED patterns were taken along the [110] & [100] MgO substrate crystal orientation, whereas (a) – (h) RHEED patterns were taken only along the [110] MgO substrate crystal orientation.

AFM results

AFM measurements were performed to study the differences in surface morphology for the $\text{Mn}_x\text{Sc}_{(1-x)}$ films. We present in Figure 2 AFM images for $\text{Mn}_x\text{Sc}_{(1-x)}$ films scanned over $5\mu\text{m} \times 5\mu\text{m}$ areas. The root mean square values (RMS) for all the AFM images presented in Figure 2 range from 2.13 nm to 24.4 nm. The lowest values are 2.13 nm, and 3.66 nm corresponding to $\text{Mn}_{0.05}\text{Sc}_{0.95}$, and $\text{Mn}_{0.35}\text{Sc}_{0.65}$ films, respectively. These RMS values agree very well with the RHEED measurements we had observed in Figure 1(c) and 1(g).

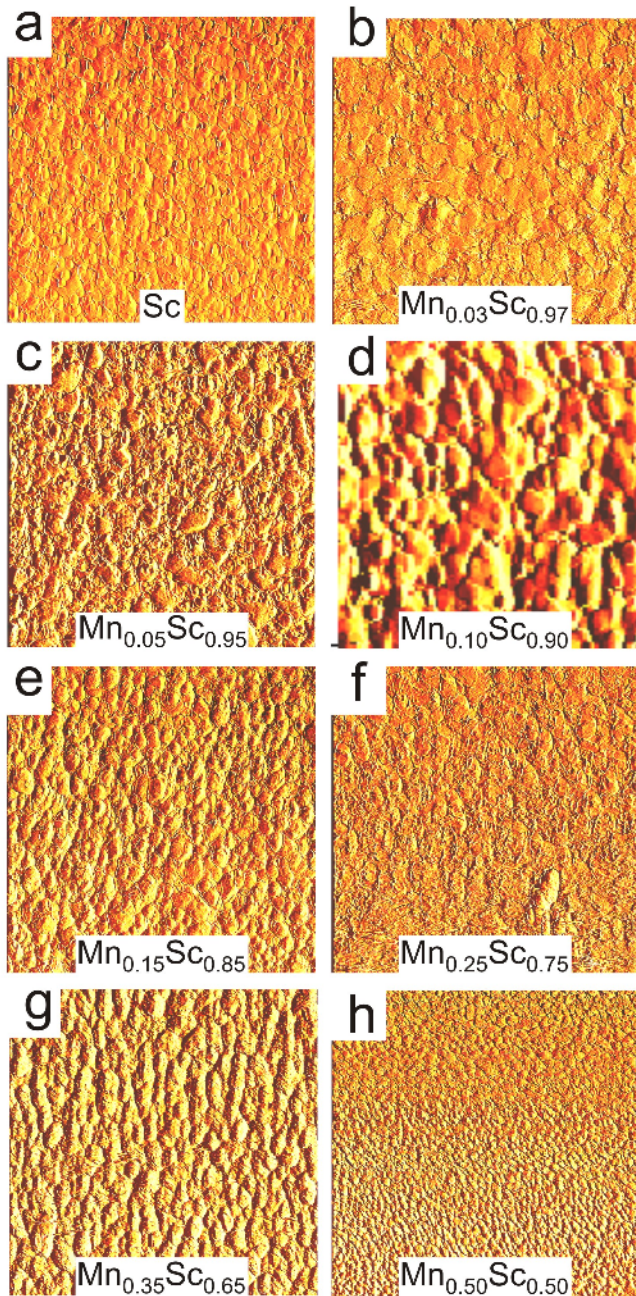


Figure 2. Atomic Force Microscopy measurements for $\text{Mn}_x\text{Sc}_{(1-x)}$ alloys at various x compositions ($0 \leq x \leq 0.5$). All images are $5\mu\text{m} \times 5\mu\text{m}$ in size.

In Figure 3 we present self-assembled nanowires measured for $\text{Mn}_{0.10}\text{Sc}_{0.90}$ [Figures 3(a) and 3(c)], and for $\text{Mn}_{0.50}\text{Sc}_{0.50}$ [Figures 3(b) and 3(d)] films. It can be seen that the nanowires in Figure 3 appear as single, double, and even triple wires connected with each other.

We found that a single nanowire can have a length of $\sim 80\,000 - 100\,000$ nm, and a width of $\sim 50 - 100$ nm. The length/width ratio of $\sim 800 - 2000$ is within the accepted nanowire range.

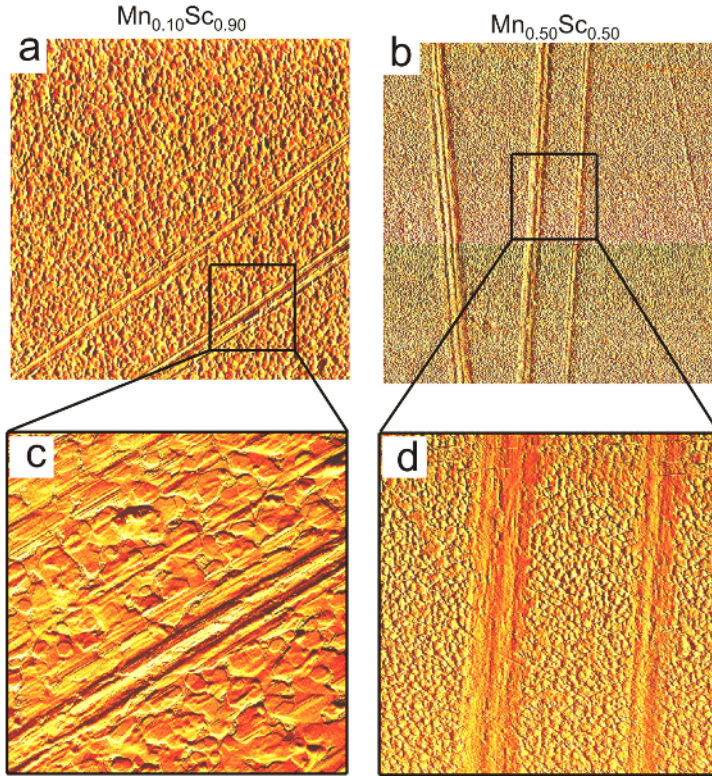


Figure 3 Atomic Force Microscopy measurements showing nanowire surface features for $\text{Mn}_x\text{Sc}_{(1-x)}$ alloys. (a) & (c) $\text{Mn}_{0.10}\text{Sc}_{0.90}$ ($20\mu\text{m} \times 20\mu\text{m}$, and $5\mu\text{m} \times 5\mu\text{m}$). (b) & (d) $\text{Mn}_{0.50}\text{Sc}_{0.50}$ ($40\mu\text{m} \times 40\mu\text{m}$, and $5\mu\text{m} \times 5\mu\text{m}$).

CONCLUSIONS

$\text{Mn}_x\text{Sc}_{(1-x)}$ films have been grown with a range of stoichiometry from $x = 0$ to $x = 0.5$. The results indicate that samples $\text{Mn}_{0.03}\text{Sc}_{0.97}$, $\text{Mn}_{0.05}\text{Sc}_{0.95}$, $\text{Mn}_{0.10}\text{Sc}_{0.90}$, $\text{Mn}_{0.25}\text{Sc}_{0.75}$, and $\text{Mn}_{0.35}\text{Sc}_{0.65}$ show a smooth, 2-dimensional growth. These alloys show very good single crystal bulk structure. Sample $\text{Mn}_{0.15}\text{Sc}_{0.85}$ MnSc shows a combination of 2 and 3-dimensional growth, which indicate alloy behavior but a rougher surface as compared to samples $\text{Mn}_{0.25}\text{Sc}_{0.75}$, and $\text{Mn}_{0.35}\text{Sc}_{0.65}$. Sample $\text{Mn}_{0.50}\text{Sc}_{0.50}$ shows a 3-dimensional and polycrystalline growth. This indicates alloy behavior, but the bulk structure is composed of many crystallites of varying size and orientation. Therefore, we can say that our MBE grown films of ~ 50 nm thickness show alloy behavior but with varying crystallinity. Future growth experiments for $x > 0.5$ will provide better understanding of such interesting alloy system. It is interesting to note that samples $\text{Mn}_{0.10}\text{Sc}_{0.90}$ and $\text{Mn}_{0.50}\text{Sc}_{0.50}$ exhibit surface self-assembled nanowires with a length/width ratio of $\sim 800 - 2000$. This is an unexpected result which needs further investigation. For future experiments, it would be very interesting to see how the surface nanowires change in length, shape, and size as the growth conditions are modified.

ACKNOWLEDGEMENTS

This collaborative work is supported by James Madison University and Ohio University (DOE-BES Grant No. DE-FG02-06ER46317 and NSF Grant No. 0730257).

REFERENCES

- [1] M.E. Drits, L.S. Toropova, and F.L. Gushchina, *Metall.* **4**, 229 (1984).
- [2] H. Okamoto, *J. Phase Equilib.* **18(4)**, 398 (1997).
- [3] G. Cacciamani, P. Riani, B. Borzone, N. Parodi, A. Saccone, R. Ferro, A. Pisch, and R. Schmid-Fetzer, *Intermetallics* **7(1)**, 101 (1999).
- [4] T. Oshima, Y. Habaram, and K. Kuroda, *Mat. Science Forum* **538-43**, 4897 (2007).
- [5] J. Gesmundo, C. deAsmundia, G. Battilana, and E. Ruedl, *Werkstoffe und Korrosion* **38**, 367 (1987).
- [6] D. Doulass, F. Gesmundo, and C. deAsmundi, *Oxidation of Materials* **25**, 235 (1986).
- [7] F. V. Buch, B. L. Mordike, A. Pisch, R. Schmid-Fetzer, *Mater. Sci. and Eng. A* **A263**, 1 (1999).
- [8] A. Pisch, R. Schmid-Fetzer, *Z. Metallkde.* **89**, 700 (1998).
- [9] J. Grobner, A. Pisch, R. Schmid-Fetzer, *J. Alloys Comp.* **317-318**, 433 (2001).
- [10] A. Pisch, F. Hodaj, P. Chaudouet, C. Colinet, *J. Alloys Comp.* **319**, 210 (2001).
- [11] H. Yang, A. R. Smith, M. Prikhodko, and W. R. L. Lambrecht, *Phys. Rev. Lett.* **89**, 226101 (2002).
- [12] H. Yang, R. Yang, A. R. Smith, and W. R. L. Lambrecht, *Surface Science* **548**, 117 (2003).
- [13] C. Constantin, K. Wang, A. Chinchore, A. R. Smith, H-J Chia, J. Markert, accepted to *Mat. Res. Soc. Symp. Proc.*